A model for the structure of the hydrated aluminum phosphate, kingite determined by ab initio powder diffraction methods

KIA S. WALLWORK,[1] ALLAN PRING,*,[1,2,3] MAX R. TAYLOR,[1] AND BRETT A. HUNTER[4]

[1]School of Chemistry, Physics and Earth Sciences, The Flinders University of South Australia, GPO Box 2100 Adelaide, South Australia 5001, Australia
[2]Department of Mineralogy, South Australian Museum, North Terrace, Adelaide, South Australia 5000, Australia
[3]Department of Geology and Geophysics, Adelaide University, North Terrace, Adelaide, South Australia 5000, Australia
[4]Neutron Scattering Group, ANSTO, PMB 1, Menai, New South Wales 2234, Australia

ABSTRACT

The crystal structure of kingite, $Al_3(PO_4)_2(F,OH)_2 \cdot 8(H_2O,OH)$, a secondary mineral from a Cambrian-Precambrian phosphate deposit at Tom's Quarry, near Kapunda, South Australia, has been determined from a powder sample using synchrotron X-ray diffraction data. The structure was determined ab initio by direct methods and refined to $R_{Bragg} = 0.022$ and $R_{wp} = 0.039$ using the Rietveld method. The triclinic structure was solved and refined in the space group $P\bar{1}$, $a = 9.377(1)$, $b = 10.113(1)$, $c = 7.138(1)$ Å, $\alpha = 97.60(1)$, $\beta = 100.88(1)$, $\gamma = 96.01(1)°$, $V = 653.0(1)$ Å^3, $Z = 2$. The structure of kingite contains finite strings of three corner sharing $Al\phi_6$ octahedra (where ϕ represents O, OH$^-$, F$^-$, or H_2O). These strings are cross-linked via PO_4 tetrahedra to produce layers that are perpendicular to [100]. The layers are linked via hydrogen bonding through H_2O located in the interlayer space. Kingite is shown to have a different stoichiometry to that reported earlier. The relationship of kingite to the structures of wavellite, $Al_3(PO_4)_2(OH)_3 \cdot 5H_2O$, and mitryaevaite, $Al_5(PO_4)_2[(P,S)O_3(OH,O)]_2F_2(OH)_2(H_2O)_8 \cdot 6.48H_2O$, are briefly discussed.

INTRODUCTION

The crystal structures of many minerals have been determined in detail using single crystal X-ray diffraction methods [see Gaines et al. 1997 and ICSD 2001 (Bergerhoff et al. 1983) for references] and this has enabled the stoichiometry and crystal chemistry of these minerals to be fully established. However, a number of minerals have, by virtue of their occurrence as microcrystalline masses, remained intractable to structure elucidation by single crystal methods. In some cases, when the symmetry is high, it has been possible to establish the crystal structure from the powder diffraction data. There remains, however, a group of microcrystalline minerals, of orthorhombic, monoclinic, and triclinic symmetry, for which crystal structures have not been determined.

The recent development of profile-fitting methods for X-ray powder diffraction analysis, together with the development of new software to accurately extract intensity data from these patterns has made possible the ab initio determination of the structure of microcrystalline inorganic compounds, for example, $Ga_2(HPO_3)_3$, (Morris et al. 1992), β-Ba_3AlF_9, (Le Bail 1993), $Bi(H_2O)_4(OSO_2CF_3)_3$, (Louër et al. 1997), $(UO_2)_3(HO_3PC_6H_5)_2 \cdot H_2O$, (Poojary et al. 1996), and recently the mineral tinticite, $Fe_6(PO_4)_4(OH)_6 \cdot 7H_2O$ (Rius et al. 2000). These developments have also been enhanced by the availability of high-intensity synchrotron sources that permit high-resolution powder diffraction patterns to be obtained from small powder samples. Louër (1998) presents a review of the methods, problems and structure solution strategies for ab initio

determination of the structure of microcrystalline compounds.

As part of an on-going program we are investigating the crystal structures of a number of phosphate and borate minerals that occur only in microcrystalline masses and we report here the crystal structure of kingite.

PREVIOUS WORK

Kingite was first described by Norrish et al. (1957) from the Fairview phosphate working near Robertstown, 150 km N.N.E. of Adelaide, South Australia, where it occurs as small fine grained nodules in soils formed from the weathering of Cambrian-Precambrian limestones during the Tertiary period (see also Mumme et al. 1984). Norrish et al. (1957) determined the formula to be $Al_3(PO_4)_2(OH,F)_3 \cdot 9H_2O$, by elemental analysis, and measured the specific gravity to be 2.27, but were unable to index the powder diffraction pattern. They noted that kingite undergoes partial dehydration between 120 and 160 °C and forms "meta-kingite," $Al_3(PO_4)_2(OH,F)_3 \cdot 4H_2O$, and they also noted a small amount of F replacing OH (less than 1 wt% F) in their elemental analysis (see below). The powder diffraction pattern was indexed with the aid of electron diffraction patterns by Kato (1970) on a triclinic cell with $a = 9.15(1)$, $b = 10.00(1)$, $c = 7.24(2)$ Å, $\alpha = 98.6(1)$, $\beta = 93.6(1)$, $\gamma = 93.2(1)°$, and $V = 652(2)$ Å^3. Kato (1970) noted that the individual platelet-like crystals of kingite are between 0.5 and 1.0 μm in diameter at the type locality. Kingite has since been found at a number of other phosphate deposits (Anthony et al. 2000), most notably at Tom's quarry near Kapunda, approximately 90 km N.N.E. of Adelaide, South Australia, where it occurs in some abundance as nodules up to 50 cm in diameter. At all localities, kingite occurs only as

---

microcrystalline masses and therefore has not been suitable for investigation by single crystal X-ray diffraction methods.

EXPERIMENTAL METHODS

A sample of kingite from Tom's quarry was obtained from the collections of the South Australian Museum, Adelaide (G12979). Wavelength dispersive electron microprobe analysis was undertaken using a Camebax SX51 instrument with a 15 kV operating voltage, 20 nA beam current, a 20 second count time, and a partially defocused beam. There was some evidence of loss of volatiles. The standards used were: Al_2O_3 (Al), hydroxylapatite (P), wollastonite (Ca), Fe_2O_3 (Fe), microcline (K), and arsenopyrite (As). The mean of eight analyses gave: P_2O_5 31.17; Al_2O_3, 36.41; CaO, 0.02; and FeO 0.61 wt%. The following elements were sought, but not found in the electron microprobe analysis: Na, K, and As. Fluorine was determined separately by microchemical analysis and the mean of four determinations gave 7.13 wt%. Combining these analyses and taking water by difference gives the following composition: $Al_{3.2}(PO_4)_2(F_{1.7}OH_{0.3})\cdot7.5(H_2O,OH)$ (calculated on the basis on two PO_4 groups).

A pure sample for powder diffraction study was scraped from the bulk sample and was loaded into a 0.3 mm diameter silica glass capillary without further crushing. The diffraction pattern was recorded using synchrotron radiation in a high-resolution powder diffractometer at the Australian National Beamline Facility (ANBF) BL-20B at the Photon Factory (KEK), Tsukuba, Japan (Garrett et al. 1995). Partial diffraction rings were collected on three adjacent image plates, located 573 mm from the axially spinning sample. Data were collected at a wavelength of 1.79475(2) Å, calibrated using an alumina reference standard (NBS 674). The data were extracted from the image plates and processed using the program Python PDA (Hester et al. 1999). The angular range of the data was 9.40–44.00°, 44.75–84.10°, and 84.30–110.40°, in steps of 0.010° of 2θ. Even though the image plates are butted together a small gap (~0.3°) occurs. For the structure analysis and refinement the RIETICA (Hunter 1998), SIRPOW.92 (Altomare et al. 1994), and GSAS (Larson and Von Dreele 1994) packages were used. Attempts to index the pattern using the cell data of Kato (1970) were unsuccessful and a new triclinic cell was obtained using the program ITO (Visser 1969). The cell parameters were refined by fitting the whole data set. A cell of higher metric symmetry could not be found by cell reduction (Le Page and Flack 1995). The unit cell from Kato (1970), although having the same volume, does not have a simple relationship to that used here, but we note that d_{100} is the same length in both cells. The space group was assumed to be $P\bar{1}$ and this choice was proved to be correct by the successful structure solution and refinement.

STRUCTURE SOLUTION AND REFINEMENT

Intensity data were extracted from the powder pattern in the form of F_{obs}^2, values using a Le Bail profile fit within RIETICA. The cell parameters, zero errors, scale factor, and peak profile parameters for each of the three histograms were refined. A pseudo-Voigt function was used to model the profile shape with coefficients being refined simultaneously whilst being constrained to be equal for all histograms. This data ex-

traction afforded 1078 reflections that were subsequently input into the direct methods program SIRPOW.92 in the form: hkl, FWHM, F_{obs}^2. A chemically plausible structural model containing all non-H atoms was obtained from the direct methods solution. The structure was then refined by the Rietveld method (Rietveld 1969), again using the pseudo-Voigt peak-shape function. Three data sets were used, one for each of the image plates. The image plates, each of which have different characteristics (Fujii et al. 1991), were read over a total time period of about 30 min. These differences were taken into account by refining a separate histogram scale factor for histograms 2 and 3; the histogram scale factor for histogram 1 was held constant. An absorption correction, based on a cylindrical sample shape, was applied before the backgrounds were fitted by Chebyshev type 1 polynomials. The number of polynomial terms used was 12, 6, and 3, for histograms 1, 2, and 3, respectively. This background function allowed the amorphous silica capillary to be properly modeled. An isotropic displacement parameter (B_{iso}) was refined for each different atom type; the O atoms were further grouped as either H_2O O atoms bound to Al, unbound H_2O, or phosphate O atoms. We note here that the displacement parameters for F are much larger than those for the other ligand atoms. We have no explanation for this. Attempts to reduce these values failed, e.g., replacing F with O produces no significant difference. The peak-shape-parameters were constrained as described for the peak extraction. The phase scale and the zero shifts were refined, as were all atomic coordinates.

The Rietveld refinement converged to R_{Bragg} of 0.022. Details of the data collection, structure solution and refinement are summarized in Table 1. The refined powder patterns are shown in Figure 1.

This solution gives a formula for kingite of $Al_3(PO_4)_2$ $(F,OH)_2\cdot8(H_2O,OH)$, which is at variance with Norrish et al. (1957). In the structure description below, where the coordinating species is undefined it is referred to as "ϕ," which represents either O, OH^-, F^-, or H_2O. We used the program PLATON (Spek 1997) to search for solvent-accessible (H_2O) voids in the structure and found none. We therefore conclude that the formula has 18 anions, two less than proposed by Norrish et al. (1957), and the number of protons in the structure is assigned to achieve charge balance. This is also in accord with the chemical analysis of kingite presented above. The presence of fluorine in kingite is discussed below.

TABLE 1. Summary of crystallographic data and refinement conditions for kingite

$Al_3(PO_4)_2(F,OH)_2\cdot8(H_2O,OH)$		μR	1.42
a (Å)	9.377(1)	no. of profile parameters	6
b (Å)	10.113(1)	no. of structural parameters	77
c (Å)	7.138(1)	no. of reflections	1047
α (°)	97.60(1)	no. of data points	9962
β (°)	100.88(1)	profile function	pseudo-Voigt
γ (°)	96.01(1)	background function	Chebyshev type I
V (Å^3)	653.0(1)	D_{obs} (g/cm^3)*	2.27(2)
D_{calc} (g/cm^3)	2.286	$χ^2$(total)	5.77
R_{Bragg}(total)†	0.022	R_{wpb}(total)‡	0.052
R_{wp}(total)†§	0.039	R_{pb}(total)‡	0.031
R_p(total)† §	0.030	R_{wpb} = $Σ((|I_o - I_c|.|I_o-I_b|)/I_o)/Σ|I_o-I_b|$	
Z	2	R_{pb} = $((Σw((I_o - I_c)(I_o - I_b)/I_o)^2)/Σw(I_o - I_b)^2)$	

* Measured by flotation in a mixture of diiodomethane and chloroform.
† For a definition of these terms see Bish and Post (1989).
‡ Calculated with background excluded.
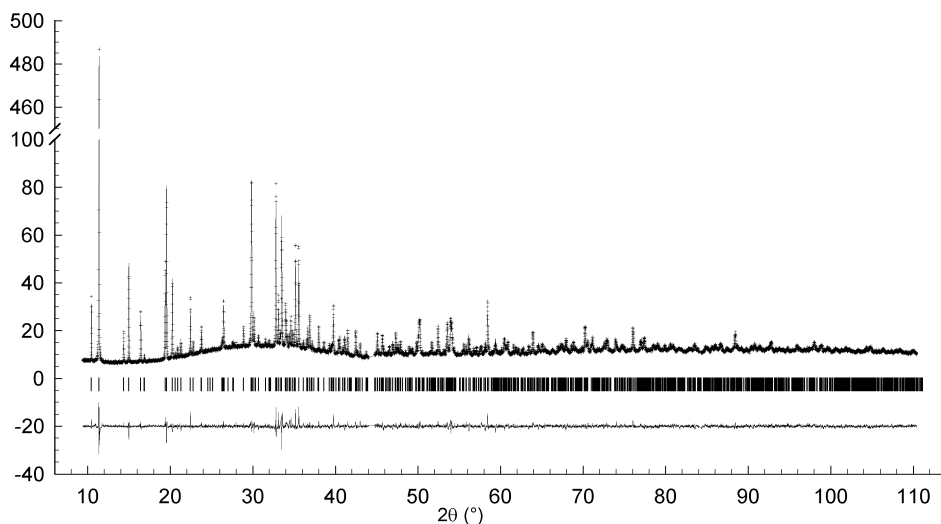§ Calculated with background included.

FIGURE 1. The powder diffraction pattern of kingite with the three histograms combined. The observed (+) and calculated (−) patterns are shown, as are the Bragg markers with the difference pattern below these. The y-scale is in arbitrary units.

The atomic coordinates and displacement parameters are listed in Table 2; selected inter-atomic distances are presented in Table 3.

STRUCTURE DESCRIPTION

The structure of kingite consists of layers, perpendicular to [100], that are composed of corner-linked tetrahedra and octahedra (Fig. 2). Within each layer discrete chains of three corner-linked $Al\phi_6$ octahedra (triads) traverse the layers parallel to [214]. The central octahedron of each triad links to the two others via opposite vertices and the latter octahedra are tilted such that two pairs of adjacent apices form edges of PO_4 tetrahedra (Fig. 3). This basic unit of three octahedra and two tetrahedra is then propagated by the four unique centers of symmetry and translational symmetry in the (100) plane to give the infinite layers shown in Figure 4. Two apices of every tetrahedron link to one triad and the other two links to two other triads, one along [010] and the other within the {010} plane. All phos-

phate O atoms are coordinated to Al, three each to Al1 and Al2, and two to Al3, leaving the remaining ligand sites to be occupied by F and O from water or hydroxide ions. The layers are linked by H bonds as indicted by interatomic distances between coordinated (F, OH⁻, and H_2O) species. Two uncoordinated water molecules in the inter-layer space are H bonded to both adjoining layers. No attempt has been made to develop a model for the H-bonding in kingite on the basis of the current refinement as a powder neutron diffraction study of deuterated kingite is in progress, from which we hope to find the hydrogen atom positions.

The Al-O/F distances in the $Al\phi_6$ octahedra range from 1.82(1) to 1.99(1) Å except for the Al1-O4 distance, which is 2.13(1) Å (Table 3). O4 is *trans* to the bridging F1 atom, which might be significant, but we note that the corresponding Al3-O13 distance is not unusual. The phosphate groups are approximately tetrahedral (P2 is better than P1), but the wide range of P-O distances, which would be expected on chemical grounds to be nearly the same, compared to the quoted standard uncertainties, is an indication of the well-known underestimation of errors by the Rietveld method. Nevertheless, the interatomic distances are similar to those reported for other aluminum phosphates. For example, in wavellite (Araki and Zoltai 1968) the

TABLE 2. Atomic coordinates, displacement parameters and atomic site occupancies for kingite

	x	y	z	B (Å²)	Occupancy
Al1	0.6816(7)	0.8460(6)	0.6141(8)	1.6(1)	1
Al2	0.4478(7)	0.7115(6)	0.1779(9)	1.6(1)	1
Al3	0.2287(6)	0.6214(6)	−0.2936(8)	1.6(1)	1
P1	0.3344(5)	0.8675(5)	0.5187(7)	1.1(1)	1
P2	0.5737(5)	0.6031(6)	−0.1866(8)	1.1(1)	1
F1*	0.6025(11)	0.7295(9)	0.3806(14)	3.6(1)	1
F2*	0.2874(12)	0.6934(9)	−0.0324(14)	3.6(1)	1
O1	0.4932(12)	0.9032(10)	0.6597(14)	1.0(1)	1
O2	0.7213(10)	0.9887(10)	0.4907(14)	1.0(1)	1
O3	0.6838(11)	0.7109(9)	0.7596(13)	1.0(1)	1
O4†	0.7621(10)	0.9823(10)	0.8760(14)	0.2(1)	1
O5†	0.8893(11)	0.8283(10)	0.6131(15)	0.2(1)	1
O6	0.3262(11)	0.7954(9)	0.3191(14)	1.0(1)	1
O7	0.5703(12)	0.6366(9)	0.0233(15)	1.0(1)	1
O8	0.3701(10)	0.5431(9)	0.2327(15)	1.0(1)	1
O9*	0.5118(11)	0.8825(9)	0.1089(13)	0.2(1)	1
O10	0.2528(11)	0.7952(9)	−0.3504(13)	0.8(1)	1
O11	0.4177(11)	0.5941(10)	−0.3091(15)	0.8(1)	1
O12*	0.0376(11)	0.6314(9)	−0.2652(13)	0.2(1)	1
O13†	0.1696(10)	0.5467(9)	−0.5565(13)	0.2(1)	1
O14†	0.1884(9)	0.4405(9)	−0.2281(14)	0.2(1)	1
O15†	0.9014(10)	0.9460(10)	0.2122(13)	1.0(1)	1
O16†	0.9723(10)	0.2906(9)	−0.1172(13)	1.0(1)	1

* Possible hydroxyl O atom.
† Possible water molecule O atom.

TABLE 3. Bond distance summary

d (Å)		d (Å)	
Al1-O1	1.99(1)	P1-O1	1.61(1)
Al1-O2	1.83(1)	P1-O2	1.60(1)
Al1-O3	1.82(1)	P1-O6	1.50(1)
Al1-O4	2.13(1)	P1-O10	1.53(1)
Al1-O5	1.98(1)		
Al1-F1	1.88(1)	P2-O3	1.56(1)
		P2-O7	1.50(1)
Al2-F1	1.82(1)	P2-O8	1.64(1)
Al2-O6	1.86(1)	P2-O11	1.54(1)
Al2-O7	1.88(1)		
Al2-O8	1.89(1)	O15-O2	2.86
Al2-O9	1.93(1)	O15-O4	2.60
Al2-F2	1.89(1)	O15-O5	2.83
		O15-O16	2.84
Al3-F2	1.87(1)		
Al3-O10	1.86(1)	O16-O7	2.88
Al3-O11	1.84(1)	O16-O12	2.76
Al3-O12	1.85(1)	O16-O14	2.70
Al3-O13	1.88(1)	O16-O15	2.84
Al3-O14	1.96(1)		

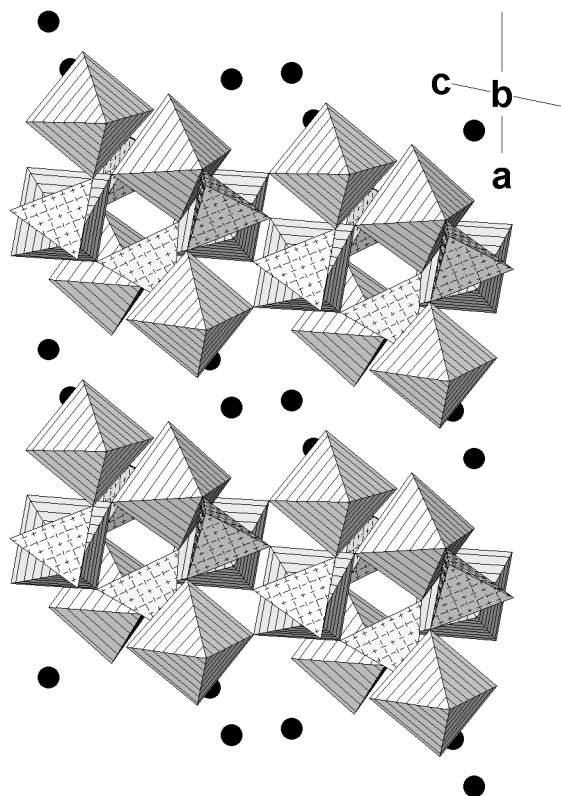**FIGURE 2.** The crystal structure of kingite viewed down **b**. The Alϕ_6 octahedra and the PO$_4$ tetrahedra are striped and crosshatched, respectively. Interlayer H$_2$O molecules are shown as black circles.

Al-ϕ distances range from 1.776(4) Å to 1.984(5) Å, with a mean of 1.89 Å, and the P-O distances range from 1.518(4) Å to 1.531(4) Å, with a mean of 1.525 Å. In the closely related mineral mitryaevaite (Cahill et al. 2001) the Al-ϕ distances range from 1.834(3) Å to 1.976(6) Å, with a mean of 1.89 Å, and the P-O distances range from 1.529(2) Å to 1.554(3) Å, with a mean of 1.54 Å. In an attempt to find a minimum with more acceptable P-O and Al-O distances the structure was refined with soft constraints on these parameters using GSAS. This refinement converged, but when the constraints were released the coordinates returned to the original solution. We have elected to present the results of the unconstrained refinement in this paper.

No attempt was made to locate H atoms or to develop an H-bonding network, but of the non-phosphate O atoms all except O9 are within a reasonable H-bonding distance of at least two potential H-bond acceptors. The bridging anions of the triads are assigned as F atoms as they are not within a reasonable H-bonding distance of potential H-bond acceptors. O9 is within H-bonding distance of only one potential acceptor and is probably an OH molecule. Each of the two interlayer water molecule O atoms (O15 and O16) are surrounded by an approximately tetrahedral environment of four O atoms [O15(O2, O4, O5, O16) 2.59–2.83 Å, subtending angles ranging between 94–127° at O15; O16(O6, O12, O14, O15) 2.70–2.84 Å, subtending angles ranging between 91–129° at O16].

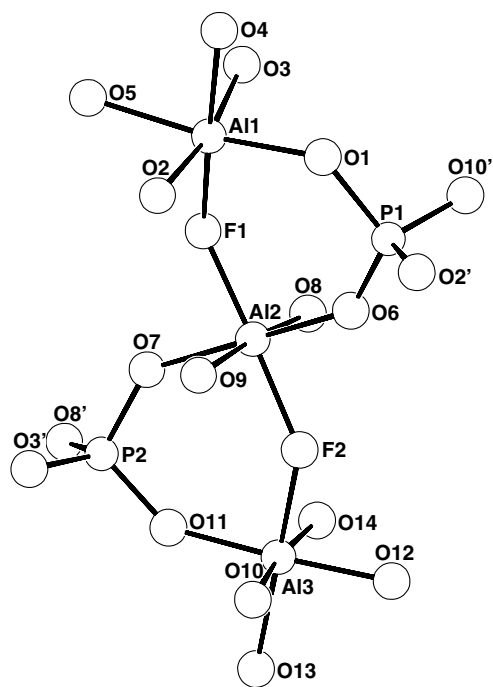We believe that the main features of the structure proposed herein

FIGURE 3. An Alf$_6$ triad with the crystallographically independent phosphate groups attached, shown with atomic labeling, where (') indicates symmetrically equivalent atoms.

for kingite are well established, although some of the details of individual interatomic distances and angles are less reliable.

REVISION OF THE KINGITE COMPOSITION

The crystal structure analysis reported here shows that kingite has nominally two less water molecules than the original formula of Norrish et al. (1957). The high water total found in the earlier analysis could be associated with the presence of F, which was greatly underestimated in the original analysis of Norrish et al. (1957). Fluorine was overlooked in our original electron microprobe analysis of the kingite used in this study, due to a faulty probe standard. Problems with the structural refinement prompted us to analyze for F, and a preliminary EDS analysis indicated the presence of significant amounts of F. Not trusting the available F electron microprobe standards, F was determined by microchemical analysis using a commercial analytical service. Four analyses were undertaken ranging from 7.07 to 7.25 (mean 7.13 wt%), giving 1.7 F atoms per formula unit and making the kingite from Tom's quarry F dominant. This finding prompted a re-examination of kingite from Fairview Quarry, Robertstown, South Australia. Microchemical analysis of some of the type material obtained from Dr. Norrish showed variable amounts of F. The four analyses gave 5.81, 5.94, 8.01, 8.29, mean 7.01 wt%. It appears that type kingite is also F dominant over OH and a formal redefinition is currently in preparation.

RELATIONSHIP TO OTHER MINERALS

The crystal chemistry and topology of phosphate mineral structures has been extensively reviewed and classified (Moore
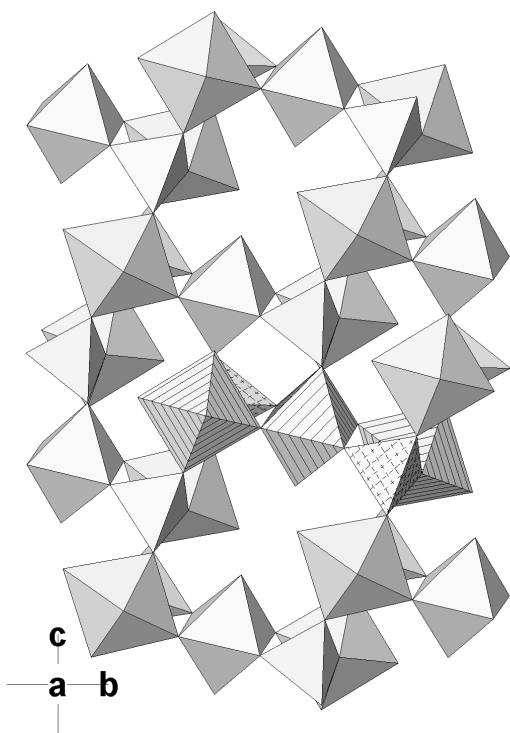
plied Crystallography, 27, 435–436.

Anthony, J.W., Bideaux, R.A., Bladh, K.W., and Nichols, M.C., Eds. (2000) Handbook of Mineralogy IV. Arsenates, Phosphates, Vanadates. Mineral Data Publishing, Tucson.

Araki, T. and Zoltai, T. (1968) The crystal structure of wavellite. Zeitschrift für Kristallographie, 127, 21–33.

Bergerhoff, G., Hundt, F., Sievers, R., and Brown, I.D. (1983) The inorganic crystal structure data base. Journal of Chemical Information and Computer Science, 23, 66–69.

Bish, D.L. and Post, J.E. (1989) Rietveld refinement of crystal structures using powder X-ray diffraction data. In D.L. Bish and J.E. Post, Eds., Modern Powder Diffraction, p. 291. Reviews in Mineralogy, Mineralogical Society of America, Washington, D.C.

Cahill, C.L., Krivovichev, S.V., Burns, P.C., Bekenova, G.K., and Shabanova, T.A. (2001) The crystal structure of mitryaevaite, $Al_5(PO_4)_2[(P,S)O_3(OH,O)]_2F_2(OH)_2(H_2O)_8 \cdot 6.48H_2O$, determined by a microcrystal using synchrotron radiation. Canadian Mineralogist, 39, 179–186.

Fujii, I., Morimoto, Y., Higuchi, Y., Yasuoka, N., Katayama, C., and Miki, K. (1991) Evaluation of X-ray diffraction data from protein crystals by use of an imaging plate. Acta Crystallographica, B47, 137–144.

Gaines, R.V., Skinner, H.C.W., Foord, E.E., Mason, B., and Rozenzweig, A. (1997) Dana's New Mineralogy, ed. 8, Wiley, New York.

Garrett, R.F., Cookson, D.J., Foran, G.J., Sabine, T.M., Kennedy, B.J., and Wilkins, S.W. (1995) Powder diffraction using imaging plates at the Australian National Beamline Facility at the Photon Factory. Review of Scientific Instruments, 66, 1351–1353.

Hawthorne, F.C. (1992) The role of hydroxyl and water in oxide and oxysalt minerals. Zeitschrift für Kristallographie, 201, 183–206.

——— (1998) Structure and chemistry of phosphate minerals. Mineralogical Magazine, 62, 141–164.

Hester, J., Garrett, R., Cookson, D., Lane, S., and Hunter, B. (1999) Python PDA. Australian National Beamline Facility local web page, http://www.ansto.gov.au/natfac/ANBF/ppda/ppdapage.html.

Hunter, B.A. (1998) Rietica—A Visual Rietveld Program. Commission on Powder Diffraction Newsletter, 20, 21.

Kato, T. (1970) Cell dimensions of the hydrated phosphate, kingite. American Mineralogist, 55, 515–517.

Larson, A.C. and Von Dreele, R.B. (1994) General Structure Analysis System (GSAS), Los Alamos National Laboratory Report LAUR 86–748.

Le Bail, A. (1993) βBa_3AlF_9, a complex structure determined from conventional X-ray powder diffraction. Journal of Solid State Chemistry, 103, 287–291.

Le Page, Y. and Flack, H.D. (1995) CREDUC. In S.R. Hall, G.S.D. King, and J.M. Stewart, Eds., Xtal3.5 User's Manual. Universities of Western Australia, Perth, Australia.

Louër, D. (1998) Advances in powder diffraction. Acta Crystallographica, A54, 922–933.

Louër, M., Le Roux, C., and Dubac, J. (1997) Ab initio structure determination from x-ray powder diffraction data of tetraaquabismuth(III) triflate obtained from the nonahydrate. Chemistry of Materials, 9, 3012–3016.

Moore, P.B. (1970) Crystal chemistry of the basic iron phosphates. American Mineralogist, 55, 135–169.

Morris, R.E., Harrison, W.T.A., Nicol, J.M., Wilkinson, A.P., and Cheetham, A.K. (1992) Determination of complex structures by combined neutron and synchrotron X-ray powder diffraction. Nature, 359, 519–522.

Mumme, I.A., Taylor, J., and Watson, K. (1984) The phosphate minerals of the Fairview rock phosphate deposit South Australia. The Australian Mineralogist, 1, 261–262.

Norrish, K., Rogers, L.E.R., and Shapter, R.E. (1957) Kingite, a new hydrated aluminum phosphate mineral from Robertstown, South Australia. Mineralogical Magazine, 31, 351–357.

Poojary, D.M., Cabeza, A., Aranda, M.A.G., Bruque, S., and Clearfield, A. (1996) Structure determination of a complex tubular uranyl phenylphosphonate, $(UO_2)_3(HO_3PC_6H_5)_2(O_3PC_6H_5)_2 \cdot H_2O$, from conventional X-ray diffraction data. Inorganic Chemistry, 35, 1468–1472.

Rietveld, H.M. (1969) Profile refinement method for nuclear and magnetic structures, Journal of Applied Crystallography, 2, 65–71.

Rius, J., Louër, D., Louër, M., Galí, S., and Melgarejo, J.C. (2000) Structure solution from powder data of the phosphate hydrate tinticite. European Journal of Mineralogy, 12, 581–88.

Spek, A.L. (1997). PLATON. Molecular Geometry Program. University of Utrecht, The Netherlands.

Visser, J.W. (1969) Fully automatic program for finding the unit cell from powder data. Journal of Applied Crystallography, 2, 89–95.

FIGURE 4. An $Al_3(PO_4)_2(F,OH)_2 \cdot 6(H_2O,OH)$ layer in kingite viewed down **a**. Stripes on the Alf_6 octahedra and crosshatching on the PO_4 tetrahedra highlight one triad within the layer.

1970; Hawthorne 1992; Hawthorne 1998). In a recent paper, Cahill et al. (2001) reported the crystal structure of mitryaevaite, $Al_5(PO_4)_2[(P,S)O_3(OH,O)]_2F_2(OH)_2(H_2O)_8 \cdot 6.48$ H_2O, and presented an overview of the crystal chemistry and hierarchical classification of phosphate and sulfate minerals. The relationship of mitryaevite to other aluminum phosphate minerals was discussed in detail and will not be reproduced here. Mitryaevite contains finite chains of five $Al\phi_6$ octahedra similar in topology to the triads of kingite. As observed in kingite, the chains in mitryaevite are cross-linked by PO_4 tetrahedra to form layers, which are in turn linked to others, by H-bonding through H_2O in the interlayer spacing.

Stoichiometrically, kingite is similar to wavellite $Al_3(PO_4)_2(OH)_3 \cdot 5H_2O$, however wavellite has a framework structure based on infinite string of $Al\phi_6$, (ϕ = O, OH, or H_2O) octahedra cross linked by PO_4 tetrahedra to form rings and channels similar to a zeolite structure (Araki and Zoltai 1968).

ACKNOWLEDGMENTS

REFERENCES CITED

Altomare, A., Cascarano, G., Giacovzzo, C., Guaglidardi, A., Burla, M.C., Polidori, G., and Camalli, M. (1994) SIRPOW.92—a program for automatic solution of crystal structures by direct methods optimized for powder data. Journal of Ap-